JOURNAL OF AIRCRAFT
Vol. 47, No. 1, January–February 2010

Longitudinal Handling Quality Analysis of a Civil Transport Aircraft Encountering Turbulence

Ming-Hao Yang* and Cjing-Shun Ho†
National Cheng Kung University, Tainan 701, Taiwan, Republic of China
C. Edward Lan‡
University of Kansas, Lawrence, Kansas 66045
and
Fei-Bin Hsiao§
National Cheng Kung University, Tainan 701, Taiwan, Republic of China

DOI: 10.2514/1.44631

The objective of this study is to analyze an aircraft's longitudinal aerodynamic characteristics and flight handling quality in the short-period mode by using flight data recorder data from a civil transport aircraft encountering turbulence. The extended Kalman filter is used to enhance the quality of the recorded data through a kinematics compatibility check and, simultaneously, estimate some unrecorded parameters. In addition, the turbofan engine's thrust is estimated with a newly established thrust model using the flight data recorder data, whereas the coefficients of aerodynamic forces and moments are evaluated with the aircraft's dynamics equations. The aircraft's longitudinal aerodynamic derivatives are then estimated by a neural network method based on radial-based functions. The results for this flight show that the short-period dynamic characteristic of the aircraft is stable, but that the flight handling quality degrades to Level 3.

Nomenclature

C_L, C_D, C_m	=	lift, drag, and pitching moment coefficient
$C_{L,D,m,x}$	=	lift, drag, and pitching moment coefficient due to state x
p, q, r	=	body rotation rate with respect to the x, y, and z axes
S	=	wing area
α	=	angle of attack or engine bypass ratio
δe	=	elevator deflection angle
δs	=	stabilizer for pitch trim
n_α	=	normal load factor per unit angle of attack
ρ	=	air density

I. Introduction

IN GENERAL, aircraft stability depicts whether the motion will diverge when the aircraft encounters the disturbance from its equilibrium state. The flight handling quality describes whether it is easy for a pilot to accomplish the assigned task at different flight phases. These two criteria are important for aircraft designers to verify that the aircraft is controllable without a huge workload for a pilot. In any aircraft accident investigation, the investigators find the clues about flight operation, aircraft motion, and system conditions from the flight data recorder (FDR). Because of the limitation of the aircraft's navigation system and the recording media capability of the FDR, sometimes there are insufficient data for investigators to perform a thorough investigation. As a result, the investigators have to use other tools, such as the training/engineering-based simulators, for further aircraft performance and stability analysis [1]. The training/engineering simulators are based on the certificated aerodynamic characteristics from the static wind-tunnel and flight-test results. These data are not capable of describing the nonlinear dynamic flight conditions in accident flight or in adverse weather encounters. Aside from the analysis of stability and performance, the investigators have not employed the flight handling quality analysis in the accident investigation to evaluate the workload. This paper wants to develop methodologies to analyze the aircraft's handling quality degradation.

Nowadays, the study of aircraft encountering atmospheric turbulence focuses on the prediction of the vertical acceleration to avoid injuries to flight attendants and passengers. Buck et al. [2] used five linear dynamic models with the aerodynamic derivatives from a simulator to predict the transient vertical acceleration. Because of the nonlinearity and unsteadiness aerodynamics, the transient response could not match the flight-test data well. According to Pollak and Lan's [3] research on calculating the effect of freestream turbulence on a delta wing by computational fluid dynamics (CFD), the lift curve slope and maximum lift coefficient degrade because of the increased boundary layer near a solid surface. Because it is not easy to model directly the atmospheric turbulence in CFD calculations, a useful alternative to determine the effect of atmospheric turbulence on aerodynamic characteristics is to extract the latter from flight data.

However, to extract aerodynamics from flight data in atmospheric turbulence, a reliable method is needed. For decades, the maximum likelihood and least-squares methods have been the dominant approaches in aerodynamic parameter identification. To accommodate more complex problems in some recent studies, the aircraft aerodynamic derivatives have been estimated by neural networks. In most of these studies, the feedforward neural networks (FFNNs) have been used to model the flight dynamics and estimate the aerodynamic derivatives directly without dealing with the noise and bias of the flight data [4]. It is a time-consuming process to find a suitable number of hidden layers, hidden nodes, types of activation functions, and iteration times to avoid the bias and noise affecting the learning results by overfitting.

Presented as Paper 5610 at the AIAA Atmospheric Flight Mechanics Conference, Chicago, IL, 10–13 August 2009; received 30 March 2009; accepted for publication 29 September 2009.

*Ph.D. Student, Department of Aeronautics, Number 1, University Road; also Associate Engineer, Aviation Safety Council, Number 200, Section 3, Beisin Road, Taipei 203, Taiwan, Republic of China; ming-hao@asc.gov.tw.

†Associate Professor, Department of Aeronautics and Astronautics, Number 1, University Road; csho@mail.ncku.edu.tw.

‡Professor Emeritus, Department of Aerospace Engineering, vortex@ku.edu. Associate Fellow AIAA.

§Professor, Department of Aeronautics and Astronautics, 66045; fbshiao@mail.ncku.edu.tw. Fellow AIAA.

In the present study, the extended Kalman filter (EKF), thrust model, and the radial-based function neural network (RBFNN) are applied to estimate the civil transport aircraft's longitudinal aerodynamic derivatives and the estimation results are used to evaluate its flight handling quality from a civil transport aircraft's FDR-recorded flight data. Because the subject aircraft encountered atmospheric turbulence, the turbulence index (TI) is used to diagnose the severity of the environment. The EKF is performed as a kinematics compatibility check. The thrust force of turbofan engines will also be estimated by a thrust model using FDR-recorded engine-related data. Then the aerodynamic coefficients are obtained and used as learning targets for the RBFNN to model the aircraft's longitudinal aerodynamic characteristics and estimate the aerodynamic derivatives. The stability and flight handling quality are evaluated by using the reduced-order longitudinal motion of the short-period mode for the aircraft response in atmospheric turbulence.

II. Aerodynamic Derivatives and Flight Handling Quality Estimation from Flight Data

A. Required Accuracy of Flight Data

For civil transport aircraft, the recorded flight data is measured or calculated in the navigation system and transmitted to the data bus in the ARINC 429 format. The flight data acquisition units collect the data and convert them into the ARINC 542, 542A, 573, 717, and 747 formats, and the data record. The error sources of the readout FDR data are from the characteristics, installation, calibration of the sensors, A/D conversion process, wiring configurations, and readout documents. Referring to International Civil Aviation Organization (ICAO) Annex 6, ED56A and ED112, the maximum tolerance range of errors for FDR data are listed in Table 1 [5]. Therefore, when investigators want to estimate unrecorded flight or further analysis based on the onboard flight data, they have to consider the bias and noise of recorded flight data.

B. Aerodynamic Derivatives Estimation

Aerodynamic derivatives are used to describe the contributions of the aerodynamic forces and moments to aircraft flight dynamics. There are three methods used to estimate the aerodynamic derivatives.

1. Approximate Mathematical Model

The approximate mathematical model is the simplest and least accurate method, and is often employed in the aircraft preliminary design to evaluate the flight stability. The values of the aerodynamic derivatives are estimated from mathematical formulas, tables, or charts that have been obtained from previous experiments and/or theoretical estimation, and may have been digitized. The most popular sources are the Engineering Sciences Data Unit and the U.S. Air Force DATCOM.

2. Wind-Tunnel Measurements

In wind-tunnel measurements, reduced-scale models of aircraft are tested. With the six-component balances, the aerodynamic forces and moments in a uniform wind condition in the tunnel can be measured. The tests are performed at different tunnel wind velocities (Reynolds numbers), angles of attack, and sideslip angles to simulate the aircraft static flight conditions. For the civil transport aircraft, the airframe designers are not specifically required to undertake the dynamic testing. Therefore, when an aircraft is in a highly dynamic situation, the nonlinear dynamic characteristics of the aircraft may be dominant, and the static test results are unreliable to describe the dynamic situation. Recently, rotary balance tests have been introduced in the dynamic wind-tunnel tests for civil aircraft. The rotary balance test is typically conducted at a very low Reynolds number, with the results used mainly in estimating the developed spin modes of general aviation and military aircraft. In addition, dynamic aerodynamic derivatives for a civil transport aircraft have also been acquired recently through the forced oscillation test at low speeds and low Reynolds numbers. However, how useful these dynamic data are in accident flight reconstruction and in describing the aircraft response in severe atmospheric turbulence encounters has yet to be verified. Therefore, for the time being it is imperative to estimate the aerodynamic derivatives from flight data for accident flight investigation.

Table 1 Error tolerance ranges for recorded flight data referring to ED112

Parameter	Accuracy	Parameter	Accuracy
Attitude	±2 deg	Normal acceleration	±0.05 *g*
Airspeed	±3%	Lat. acceleration	±0.05 *g*
Ground speed	Depend	Long. acceleration	±0.05 *g*
Drift angle	Depend	Total air temperature	±2°C
Wind speed	Depend	AOA	Depend
Wind dir.	Depend	Lat./Long.	Depend

3. Flight-Test Measurements

In flight-test measurements, a parameter identification method is still needed. In the late 1960s, flight-test measurements were developed at NASA and some flight-test research centers [6]. As the computer calculation speed and system identification technology has improved, the aerodynamic derivative identification method has also evolved in complexity. The calculation method started from the least squares to the Newton–Raphson and then evolved to the maximum likelihood [7]. The aerodynamics to be identified has progressed from a linear to a nonlinear one. Today, the maximum likelihood is still widely used in this field [8]. No matter which identification method is used, the estimation is mostly based on a small disturbance theory, by building up the aerodynamics from the equilibrium or trim at a specific flight condition. The aerodynamic derivatives from this method represent the quasi-steady values at the equilibrium states. Note that abnormal flight conditions outside the flight envelope are not flight tested, so that the flight-test data are still inadequate for accident investigation.

The aerodynamic characteristics derived from the aforementioned methods are reasonable in the normal operation. When an aircraft encounters adverse weather, such as severe atmospheric turbulence, or in a loss-of-control situation, the associated aerodynamics is expected to be highly nonlinear and dynamic in nature. Therefore, an appropriate identification method must be capable of handling more complex phenomena. One such method is based on an artificial intelligence technique [9].

C. Flight Handling Qualities

The flying and handling qualities of an aircraft are described as the acceptability and suitability for safe and efficient control by pilots to execute flight tasks. These two qualities are described qualitatively and are formulated in terms of pilot opinions. From the pilot's point of view, the flying quality is regarded as how well an aircraft responds to the pilot's command. The two qualities are interdependent and are probably inseparable. Therefore, the flying and handling qualities are frequently referred to as flight handling quality. The pilot's perception of the flight handling quality of an aircraft is influenced by many factors, such as the stability, control, and dynamic characteristics of the airframe; flight control system dynamics; response to atmospheric disturbance; and cockpit design. The engineering criteria of the flight handling qualities include a low-order equivalent system/control anticipation parameter (CAP), bandwidth, time response, dropback, Nichols Chart, and Neal–Smith. The aforementioned criteria are based on analysis in the frequency domain and transfer functions, verified on the ground-based simulators, and flight-tested inside the flight envelope. The present analysis focuses on the aircraft aerodynamics and flight dynamics, and flight handling quality in encountering atmospheric turbulence. The parameters, used to describe the motion of aircraft,

are estimated from the recorded flight data to represent the real dynamic situations of the aircraft.

When the aircraft encounters atmospheric turbulence, the buffeting of the airframe and its effect on the pitching attitude and angle of attack may cause the aerodynamics to be highly nonlinear or, in the worst situation, the aircraft becoming unstable. With regard to the aircraft flight dynamics, the resulting aerodynamic environment may cause the pilots to lose control of the longitudinal short-period mode of aircraft. Therefore, in the present study the longitudinal short-period mode is analyzed based on the damping ratio and undamped natural frequency of the reduced-order longitudinal equations of motion. The CAP index and normal load factor per unit angle of attack, n_α, are used to depict the degradation of the flight handling quality.

III. Methodology

In the present study, the bias and noise of the recorded flight data of a civil transport aircraft are filtered out by performing a kinematics compatibility check through EKF. In this way, the unrecorded flight data, such as sideslip angle, three-dimensional winds, etc., are derived or improved in data quality. The severity of encountering atmospheric turbulence is diagnosed by the EDR index, evaluated by flight data. Then, the thrust forces are derived from the thrust model and the FDR-recorded flight data for turbofan engines. Once the flight data and thrust forces are estimated, the aerodynamic force and moment of the aircraft on the body axes are derived by plugging the flight states and thrust forces into the nonlinear flight dynamic equations. The aerodynamic forces are then translated into wind axes. In most cases when an aircraft encounters atmosphere turbulence, the onboard passengers and flight crew suffer injuries because of the rapid bumping of the aircraft in a longitudinal motion. Therefore, this study focuses on the analysis of the aircraft's longitudinal characteristics. To analyze the degradation of longitudinal aerodynamic characteristics, the longitudinal aerodynamic derivatives are modeled by the RBFNN. After obtaining the longitudinal aerodynamic derivatives, the damping ratio, undamped natural frequency, CAP, and n_α are estimated and used to evaluate the longitudinal flight handling quality. In the following paragraphs, the EKF, atmospheric turbulence strength identification, thrust model, and radial-based function neural network employed in this study will be discussed.

A. Extended Kalman Filter

The EKF can be applied to the nonlinear optimal estimation. It uses the system's observations, measurements, system's dynamics, and measurement's dynamics to estimate the noise and bias embedded in the measurements and estimate system parameters. EKF applies sequential and recursive processes by linear minimum variance theory [10]. The nonlinear stochastic differential and measurement equations map the states and measurements at time $k-1$ to k can be described as

$$X_K = f(X_{K-1}, k-1) + g(X_{k-1}, k-1)w_{k-1} \qquad k = 0, 1, 2.$$
$$Z_k = h(X_K, k) + v_k \qquad k = 1, 2 \tag{1}$$

where w_k and v_k denote the processing and measurement noise of the system.

The a priori error covariance matrix, P_k^-, is defined as the difference between the true state (X_k) and the predicted state at time k, and can be formed as

$$P_k^- = E[(X_k - \widehat{X}_k(-))(X_k - \widehat{X}_k(-))^T] = \Phi_{k-1}P_{k-1}\Phi_{k-1}^T + G_{k-1}Q_{k-1}G_{k-1} \tag{2}$$

where $\widehat{X}_k(-)$ is a previous estimate of the system state at k, derived from the estimated state at time $k-1$ from the state transition matrix

$$\Phi_{k-1} = \left.\frac{\partial f(x, k-1)}{\partial x}\right|_{x=\widehat{x}_{k-1}} \tag{3}$$

where Q is the expected value of processing noise, defined as $E(w_k w_k^T)$.

The EKF uses the Kalman filter gain, K, to adjust and update the system state at time k by the $\widehat{X}_k(-)$, and the system predicted measurements and measured values.

$$\widehat{X}_k(+) = \widehat{X}_k(-) + K(Z_k - \widehat{Z}_k) \tag{4}$$

The Kalman filter gain is a function of an a priori error covariance matrix, system measurement dynamic matrix,

$$\left(H_k = \left.\frac{\partial h(x, k-1)}{\partial x}\right|_{x=\widehat{X}_{k-1}}\right) \tag{5}$$

and measurement noise ($R_k = E(v_k v_k^{-1})$). The final expression for the gain is

$$K = P_k^- H_k^T (H_k P_k^- H_k^T + R_k)^{-1} \tag{6}$$

Through this calculation process, the error covariance matrix is minimized to result in

$$P_k = (I - KH_k)P_k^{-1} \tag{7}$$

The flight data for this study are divided into two groups: inertial and pneumatic. The pneumatic data are corrected by quasi nonhydrostatic to obtain the true airspeed. To verify that the noise and bias of estimated states are removed, the estimated results are used to recalculate the states of aircraft by plugging them into the nonlinear flight kinematics equations, and observe whether the estimated results are converging to and approaching the recorded flight data. After the aforementioned procedures are done, the wind speed and wind direction are calculated from the difference between the ground speed and true airspeed.

B. Atmospheric Turbulence Strength Identification

The atmospheric turbulence strength can be estimated by the fluctuation of vertical acceleration, the EDR, and the vertical wind variation [11]. The instantaneous peak and root mean square values can be used to indicate the severity of atmospheric turbulence in these three indexes. According to ICAO and World Meteorological Organization documents in 2006, the automatic pilot reporting system is based on TI to define the severity of atmospheric turbulence. The value of TI is defined in terms of the instantaneous and rms values of EDR, and the severity is related to them as follows [12]:

Severe: TI = 15 to 27, Peak EDR > 0.5

Moderate: TI = 6 to 14, 0.3 < Peak EDR < 0.5

Light: TI = 1 to 5, 0.1 < Peak EDR < 0.3

None: TI = 0, Peak EDR < 0.1

EDR describes the dissipation of turbulence kinetic energy, and the value of EDR can be estimated from the aircraft response to the vertical wind in the frequency domain as follows:

$$\phi_{\dot{Z}}(f) = |H_{\dot{Z}}(f)|^2 \phi_w(f) \tag{8}$$

where $\phi_w(f)$ is the vertical wind component of turbulence at frequency f, $|H_{\dot{Z}}(f)|$ is the transfer function of aircraft response, and $\phi_{\dot{z}}(f)$ is the aircraft response in vertical acceleration. Using von Karman's power spectral density, and the integral for the rms, EDR (ε) can be approximated as

$$\varepsilon^2(t) = \frac{\sigma^2(t)}{0.7V^{2/3}I'(t)} \tag{9}$$

C. Thrust Model for Turbofan Engine

In reality, the thrust force should vary with dynamic flight variables and turbulence strength. However, the functional relation requires further research and is beyond the scope of this paper. For the present purpose, it is assumed that thrust affects only the aircraft pitch trim, but not the aerodynamic derivatives, the slopes of aerodynamic forces and moments. The engine thrust in this study is calculated from a static thrust model to be developed and the FDR data. The recorded data includes the engine pressure ratio (EPR), engine exhaust temperature, N1 and N2. The nozzle exit temperature is assumed to be the same as the FDR-recorded exhaust gas temperature (EGT). As a result, the time lag between the pilot command, engine response, and engine health problems are ignored.

The subject aircraft is equipped with PW4159 turbofan engines. The bypass ratio (α) and the fan pressure ratio (FPR) for these engines are 4.8 and 1.73, respectively. The thrust force of the turbofan engine is calculated by using the momentum principle with contributions from the core engine and fan section and can be shown to be [13]

$$\frac{T}{\dot{m}_0} = \frac{a_0}{1+\alpha}\left[\frac{V_{ec}}{a_0} - M_{a0} + \alpha\left(\frac{V_{ef}}{a_0} - M_{a0}\right)\right] \tag{10}$$

where $\dot{m}_0$ is the mass flow rate, M_{a0} is the flight Mach number, a_0 is the flight speed, V_{ec} is the effective exhaust velocity in the core flow, V_{ef} is the effective exhaust velocity in the fan flow. These two velocities are estimated from the Eq. (11) and (12)

$$\left(\frac{V_{ec}}{a_0}\right)^2 = \frac{2\text{EGT}}{T_0(\gamma-1)}\left[\left(\text{EPR} * \frac{P_{t0}}{P_0}\right)^{\gamma-1/\gamma} - 1\right] \tag{11}$$

$$\left(\frac{V_{ef}}{a_0}\right)^2 = \frac{2}{\gamma-1}\left[\left(\frac{P_{t0}}{P_0}\frac{\text{FPR}}{N_2}\right)^{\gamma-1/\gamma} - 1\right] \tag{12}$$

P_{t0}/P_0 is the total to static pressure ratio of the freestream before entering to the engine, and T_0 is the static temperature of the freestream.

D. Radial-Based Function Neural Network

The learning mechanism for the RBFNN is based on weighting the distance between the input and the centers of the radial-based function to fit the desired output. It is similar to the definition of quasi-steady aerodynamic derivatives, which were defined relative to the equilibrium flight condition. The centers of the radial-based function for various segments of flight data were similar to the equilibrium states at different flight phases or segments.

RBFNN is a type of feedforward NN. The structure of RBFNN consists of three layers: input, hidden layer, and output layer. The hidden layer is a radial-based function and measures the distance between the input and weighted distance. The weighted distances are summed and compared to the target value [14,15]. These depictions are written as

$$y(p) = \sum_{j=1}^{M} w_j * \phi(\|x(p) - c_j\|) + w_0 \tag{13}$$

where $y(p)$ is the learning result of the RBFNN at time p, $\phi(\|x - c_j\|)$ is the radial-based function, $x(p)$ is the input vector of the flight state, c_j is the center of the jth neuron at the hidden layer, w_j is the weighting, and w_0 is the bias. In this study, the Gaussian function is used as the radial-based function:

$$\phi(\|x(p) - c_j\|) = \exp\left[-\frac{\|x(p) - c_j\|^2}{2\sigma_j^2}\right] \tag{14}$$

where σ_j is standard deviation, defined as the shape of the radial-based function.

The steepest learning rule is applied to the RBFNN. In the learning process, w_j, c_j, and σ_j in Eq. (15) have to be corrected with the learning rate ($\eta_{1\sim3}$) to minimize the learning error.

$$\begin{aligned}
\Delta w_j(p) &= \eta_1 e(p)\phi(\|x(p) - c_j(p)\|) \\
\Delta c_j(p) &= \eta_2 \frac{w_j(p)e(p)}{\sigma_j^2(p)}\phi(\|x(p) - c_j(p)\|)(x(p) - c_j(p) \\
\Delta \sigma_j(p) &= \eta_3 \frac{w_j(p)e(p)}{\sigma_j^3(p)}\phi(\|x(p) - c_j(p)\|)(x(p) - c_j(p))^2
\end{aligned} \tag{15}$$

The nonlinearity and accuracy of RBFNN are controlled by the numbers of neurons and their centers. When the number of centers is increased, the learning results will be mired in the local minimum of the learning error. Therefore, the suitable initial value of the centers of the radial function and weightings are determined by the fuzzy c-means (FCM) and orthogonal least-squares (OLS) algorithm. In this study, the initial values of the RBFNN for the lift and drag coefficients are determined by the FCM and the pitching moment coefficient is set by the OLS. The FCM is a method of clustering, allowing a piece of data to belong to more than one cluster. The partitioning of FCM is carried out through an iterative optimization of the objective function by updating the membership and the center of the jth neuron. The center point is not necessary from the input state of the flight data. Instead, every input datum is considered as the center of the jth neuron for the OLS method. The OLS method will use orthogonal least squares to minimize the objective function through repeating orthogonal least-squares calculations to choose the centers of the neuron. In this way, the OLS is a time-consuming process to find the suitable initial condition for the RBFNN.

E. Decoupled Longitudinal Equations of Motion

Basically, the linearized decoupled aircraft longitudinal dynamics are described by the following three equations of motion:

$$\begin{aligned}
m\dot{u} - \overset{o}{X}_{\dot{w}}\dot{w} &= \overset{o}{X}_u u + \overset{o}{X}_w w + (\overset{o}{X}_q - mW_e)q - mg\theta\cos\theta_e + \overset{o}{X}_\eta \eta \\
m\dot{w} - \overset{o}{Z}_{\dot{w}}\dot{w} &= \overset{o}{Z}_u u + \overset{o}{Z}_w w + (\overset{o}{Z}_q - mU_e)q - mg\theta\sin\theta_e + \overset{o}{Z}_\eta \eta \\
I_y\dot{q} - \overset{o}{M}_{\dot{w}}\dot{w} &= \overset{o}{M}_u u + \overset{o}{M}_w w + \overset{o}{M}_q q + \overset{o}{M}_\eta \eta
\end{aligned} \tag{16}$$

where the X, Z, and M are the axial force for the drag, normal force, and pitching moment, respectively. The subscript states for the $\overset{o}{X}$, $\overset{o}{Z}$, and $\overset{o}{M}$ are the dimensional aerodynamic derivatives related to the states on the body axes.

With Φ defined in the following, Eq. (17) is multiplied by Φ^{-1} and rearranged in form of $\dot{x}(t) = Ax(t) + Bx(t)$ to result in

$$\Phi = \begin{bmatrix} m & -\overset{o}{X}_{\dot{w}} & 0 & 0 \\ 0 & (m - \overset{o}{Z}_{\dot{w}}) & 0 & 0 \\ 0 & -\overset{o}{M}_{\dot{w}} & I_y & 0 \\ 0 & 0 & 0 & 1 \end{bmatrix}$$

$$\begin{bmatrix} \dot{w} \\ \dot{q} \\ \dot{\theta} \end{bmatrix} = \begin{bmatrix} z_w & z_q & z_\theta \\ m_w & m_q & m_\theta \\ 0 & 1 & 0 \end{bmatrix}\begin{bmatrix} w \\ q \\ \theta \end{bmatrix} + \begin{bmatrix} z_\eta \\ m_\eta \\ 0 \end{bmatrix}\eta \tag{17}$$

where z_w, z_q, z_θ, m_w, m_q, and m_θ are defined as the concise form of aerodynamic derivatives. The short-period mode is typically a damped oscillation in pitch about the body y axis in normal flight conditions. The main motion variables include the angle of attack, the pitch rate, and the pitch angle. If we assume the aircraft is in steady level flight, the equation of motion is therefore

$$\begin{bmatrix} \dot{w} \\ \dot{q} \end{bmatrix} = \begin{bmatrix} z_w & z_q \\ m_w & m_q \end{bmatrix}\begin{bmatrix} w \\ q \end{bmatrix} \tag{18}$$

Equation (19) is similar to a second-order vibration equation, with the natural frequency and damping ratio given by

$$\omega_{sp} = \sqrt{(m_q z_w - m_w z_q)}, \qquad 2\zeta_{sp}\omega_{sp} = -(m_q + z_w) \tag{19}$$

The short-period transfer functions describing the pitch rate, angle of attack, and normal acceleration response to an elevator control input, respectively, are given as follows:

$$\frac{\dot{q}(s)}{\eta(s)} = \frac{m_\eta s(s - z_w)}{(s^2 - (m_q + z_w)s + m_q z_w - m_w z_q)} \tag{20}$$

$$\frac{a_z(s)}{\eta(s)} = \frac{m_\eta z_w u_0}{(s^2 - (m_q + z_w)s + m_q z_w - m_w z_q)} \tag{21}$$

$$\frac{\alpha(s)}{\eta(s)} = \frac{\frac{z_\eta}{u_0}(s + u_0 \frac{m_\eta}{z_\eta})}{(s^2 - (m_q + z_w)s + m_q z_w - m_w z_q)} \tag{22}$$

For the flight handling quality criteria, the normal load factor per unit angle of attack (n_α) and CAP are defined as follows [16]:

$$n_\alpha = \frac{n_z(t)}{\alpha(t)}\bigg|_{ss} = -\frac{z_w u_0}{g} \equiv \frac{u_0}{gT\theta_2} \tag{23}$$

$$\text{CAP} = \frac{\dot{q}(0)}{n_z(\infty)} = -\frac{g\omega_{sp}^2}{z_w u_0} = \frac{g\omega_{sp}^2 T_{\theta_2}}{u_0} \tag{24}$$

IV. Numerical Results

A. Turbulence Strength Identification

The rms time window of the EDR was 5 s. The instantaneous peak and rms of the EDR are denoted by EDR_{INST} and EDR_{RMS} spatially. The results are shown in Fig. 1. They show that the aircraft encountered the turbulence the first time at 240–270 s. The most severe turbulence at the first time is at 256 s. At that time, the EDR_{INST} is 0.557, the EDR_{RMS} is 0.436, and the TI is 19. Therefore, the encountered turbulence is classified as "severe."

B. Estimation of Flight Data and Thrust Force

To estimate the unrecorded flight data and remove the noise and bias of the recorded flight data, the EKF was used as a kinematics consistency check, as indicated earlier. The state transition and measurement matrix for EKF are the partial differential equations of nonlinear kinematics equations of flight dynamics. The thrust force is estimated by inserting the FDR-recorded flight data and the dimension of the engine into Eqs. (10–12) of the thrust model. Then the aerodynamic coefficients are estimated from the dynamic equations of motion. The time history for the lift coefficient (C_L), drag coefficient (C_D), side force coefficient (C_Y), pitching moment coefficient (C_m), rolling moment coefficient (C_l), and yawing moment coefficient (C_n) are shown in Fig. 2.

The horizontal wind speed and direction with a 0.25 sampling rate are also available from the data recorder but without the vertical wind information. The sampling rate is not enough to know the turbulence wind field. Through the EKF, the three-dimensional wind field could be derived with a higher sampling rate. Figure 3 depicts the estimation results of the three-dimensional wind field along the flight track and the recorded horizontal wind information at the navigation axis. According to the calculated three-dimensional wind field, the minimum and maximum values of wind speed normal to the horizontal plane are −9.8 and 36 kt, respectively, (see Fig. 3), and the covariance for the derived and recorded horizontal wind speed is about 96.5%.

C. Aircraft Longitudinal Aerodynamic Derivatives

The aerodynamic derivatives are estimated by the RBFNN. The input vector for the RBFNN is the flight states, estimated by the EKF. The longitudinal aerodynamic coefficients are used as the learning targets. In this way, the mathematical descriptions of the aircraft's longitudinal forces and moments are not necessary to find in this study. In this way, some coupling and high-order terms of the aerodynamic derivatives could be estimated. Furthermore, the aerodynamic derivatives are based on the wind axes, instead of the body axes, for the aerodynamic-forces-related derivatives, because it is much easier to judge whether the structure of RBFNN is correct. The primary focus of this paper is to evaluate the handling quality of the civil transport aircraft by the aircraft's longitudinal reduced-order motion. Therefore, the coupling and high-order terms of aerodynamic derivatives will not be examined.

The input states for the longitudinal aerodynamic forces coefficients are affected by Mach number (Ma) time rate of magnitude of the vertical wind component (w_w), rotational rates at the body axes (p, q, r) and their time rates ($\dot{p}$, $\dot{q}$, $\dot{r}$), angle of attack (α) and its rate ($\dot{\alpha}$), sideslip angle (β) and its rate ($\dot{\beta}$), and the stabilizer for pitch trim (δ_s). Those parameters are the input states for the RBFNN. The elevator effects on C_L and C_D are ignored in the present study. On the other hand, for the pitching-moment-related derivatives, the elevator deflection is considered as an important contributing variable. The longitudinal aerodynamic coefficients of these variables are modeled by RBFNN. The longitudinal aerodynamic derivatives will be used to evaluate the stability and flight handling quality. The estimated results of aerodynamic derivatives are depicted in Fig. 4.

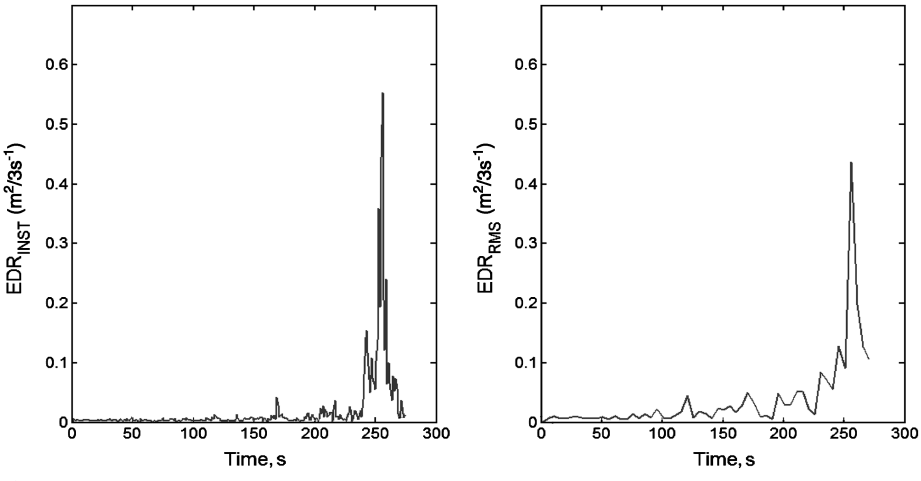

a) b)

Fig. 1 EDR: a) instantaneous peak value, and b) rms value.

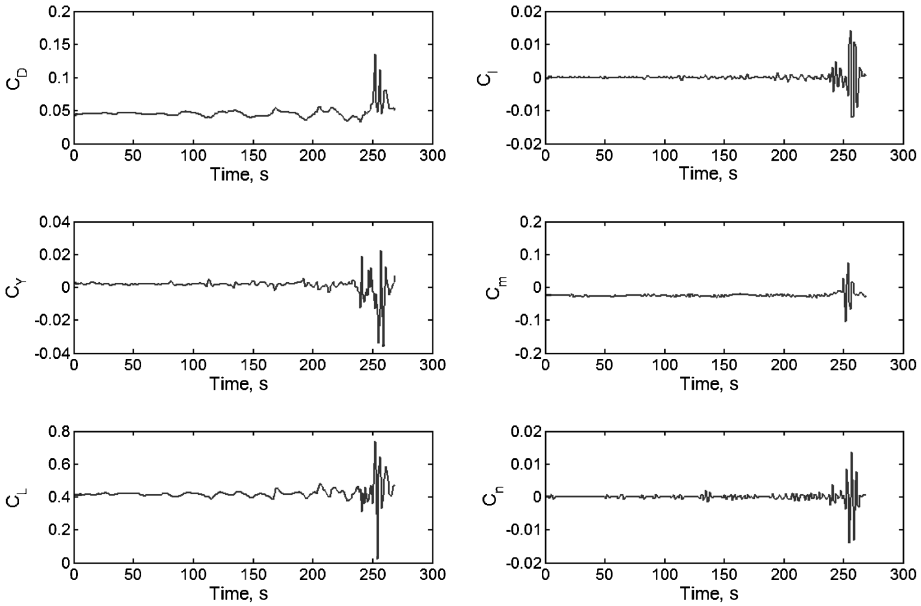

Fig. 2 Time history for the aerodynamic coefficients.

About a quarter of the whole flight data is used in the learning phase and then the whole flight data are used to validate whether the learning results of RBFNN could represent the longitudinal dynamics of aircraft. The initial values of the centers of the radial-based function and weightings are determined by the FCM algorithm for the learning of the lift and drag coefficients and the OLS method is applied for the learning of the pitching moment modeling. After the learning results from the network structure can track the target values, then the aerodynamic derivatives are estimated. The aerodynamic derivatives estimation from RBFNN is similar to performing the sensitivity analysis for the RBFNN. The sensitivity is used to check the degree of the learning result being affected by specific input parameters. If the longitudinal aerodynamic coefficient due to a specific state is $x_i(p)$, and the increase is $\Delta x_i(p)$, then the total input should be $x(p) + \Delta x_i(p)$ and its learning result from the RBFNN is $y(p)|_{x(p)+\Delta x_i(p)}$. Therefore, the longitudinal aerodynamic coefficient due to the specific state could be derived as follows:

$$\frac{y(p)|_{x(p)+\Delta x_i(p)} - y(p)}{(x(p) + \Delta x_i(p)) - x(p)} = \frac{y(p)|_{x(p)+\Delta x_i(p)} - y(p)}{\Delta x_i(p)} \tag{25}$$

The nonlinearity of RBFNN is affected by the number of neurons in the hidden layer. As the number of neurons increases, it will make a better fit between the learning results and targets and also increase the sensitivity of the RBFNN and affect the aerodynamic derivatives. The nonlinearity will make the structure of the network converge to the local minimum. The situation not only increases the standard deviation of the aerodynamic derivatives but also affects the values of the aerodynamic derivatives. Therefore, the suitable number of neurons is judged by the fitting results and the magnitude and the sign of the aerodynamic derivatives. Because the actual aerodynamic derivatives for the subject airplane are not available, the following results for the Convair 880 and Boeing 747, listed in Table 2 [17], will be used for comparison, because the weight of the subject aircraft falls between these two types of aircraft.

1. *Derivatives of Lift Coefficient*

Before encountering atmospheric turbulence, the subject aircraft was operating normally in cruise conditions. The flight level, which is the nominal altitude in feet and divided by 100, was 330, and the Ma was 0.78. Before encountering atmospheric turbulence, the average values of $C_{L\alpha}$, $C_{L\delta s}$, $C_{L\beta}$, and C_{LMa} are 4.47, 0.189, −0.016, and −0.0098, respectively. Compared to the results in Table 2, the values of $C_{L\alpha}$ and $C_{L\delta e}$ for the Convair 880 are 4.8 and 0.19 at a Mach number of 0.8, and the values for the Boeing 747 are 5.5 and 0.33, respectively. Therefore, the estimated results are reasonable and are in the range for these two types of aircraft in cruise conditions.

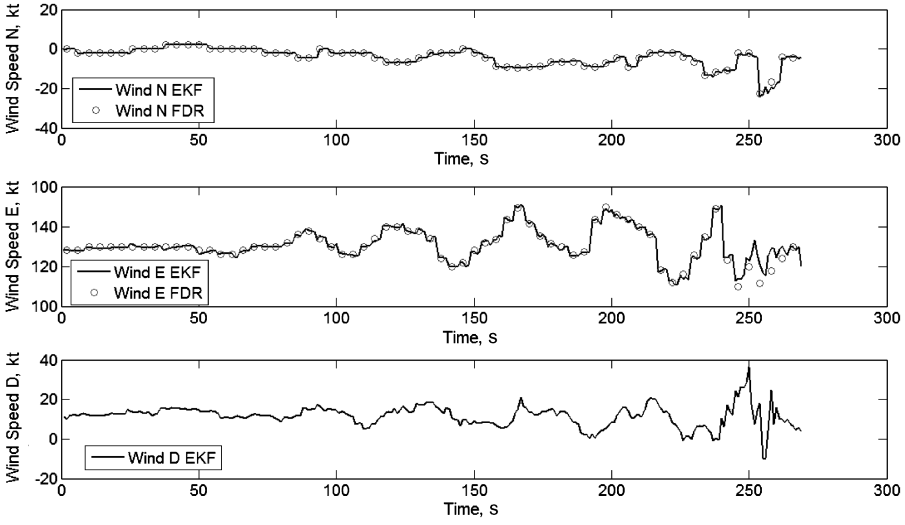

Fig. 3 Estimated results for the three-dimensional wind fields.

Table 2 Some the longitudinal aerodynamic derivatives of Convair 880 and Boeing 747

	$C_{L\alpha}$	$C_{D\alpha}$	$C_{m\alpha}$	$C_{m\delta e}$	C_{mq}	$C_{L\delta e}$
			Convair 880			
$Ma = 0.8$	4.8	0.15	−0.65	−0.57	−4.5	0.19
			Boeing 747			
$Ma = 0.9$	5.5	0.47	−1.6	−1.2	−25	0.3

When the subject aircraft flew into the atmospheric turbulence, $C_{L\alpha}$ varied from 5.17 to 0.41. The value of $C_{L\delta s}$ varied from 0.189 to 0.001. From these results, the effectiveness of lift force due to the stabilizer for this case was decreasing. Therefore, the control power of the stabilizer, $C_{m\delta s}$, was expected to decrease as well. The lift coefficient related derivatives are shown in Fig. 4.

2. Derivatives of Drag Coefficient

Before encountering the atmospheric turbulence, the average values of $C_{D\alpha}$, $C_{D\delta s}$, and $C_{D\beta}$ were 0.48, 0.0001, and −0.003, respectively. In Table 2, the values of $C_{D\alpha}$ for Convair 880 and Boeing 747 are 0.15 and 0.47, respectively, at a Mach number of 0.8. Therefore, the estimated results are in the range for these two types of aircraft in cruise conditions. The magnitude of drag derivatives were also very small except for $C_{D\alpha}$. As a result, these small terms are neglected in the following study.

With the aircraft in atmospheric turbulence, the values of $C_{D\alpha}$ varied in the range of 0.6–0.28. The drag coefficient derivative with stabilizer angle is not significant. The drag coefficients related derivatives are depicted in Fig. 5.

3. Derivatives of Pitching Moment Coefficient

Figure 6 shows some estimated derivatives of the pitching moment coefficient. Before encountering atmospheric turbulence, the average value of $C_{m\alpha}$ is −0.337, $C_{m\delta s}$ is −2.79, $C_{m\delta e}$ is −1.12, and C_{mq} is −5.56. In [12], $C_{m\delta e}$ is −0.58 at a Mach number of 0.8 for the Convair 880, whereas the value for the Boeing 747 at a Mach number of 0.9 is −1.2. When the aircraft encountered atmospheric turbulence, the values of $C_{m\alpha}$, $C_{m\delta s}$, and $C_{m\delta e}$ ranged from −0.02 to −0.44, −2.92 to −0.05, and −1.64 to 0.11, respectively. It should be noted that the pitching moment derivatives depend on the location of the center of gravity.

The pitching moment coefficient due to angle of attack represents the static stability of the aircraft, the value being negative during normal operation. For the severe atmospheric turbulence case, although the aircraft is still statically stable, the static stability was decreasing and degraded by up to 96%. In addition, $C_{m\delta s}$ and $C_{m\delta e}$, representing the pitching control power from the stabilizer and elevator, also decreased in magnitude. In the present study, the sign for $C_{m\delta e}$ is changed from negative to positive. Referring to Eqs. (20–22), the sign change of $C_{m\delta e}$ means a significant and opposite phase delay in the elevator control relative to the motion. If the pilot applies control to

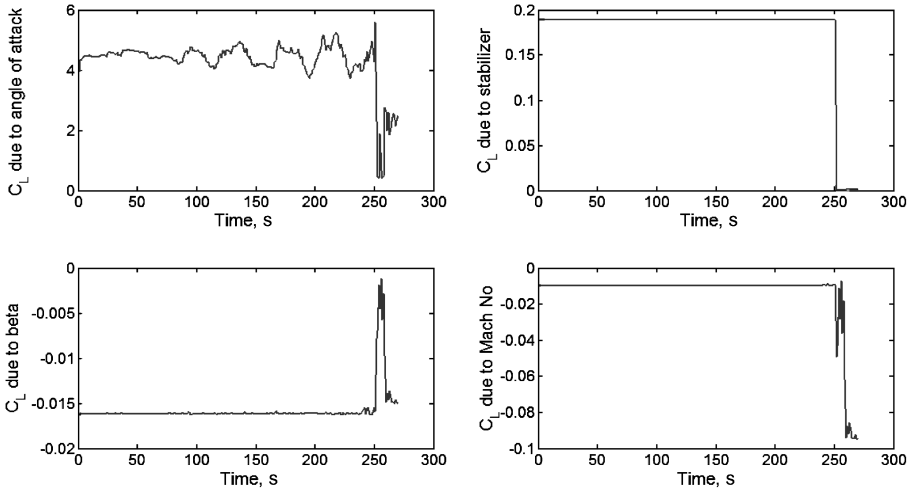

Fig. 4 Some of the lift-coefficient-related aerodynamic derivatives estimated by RBFNN.

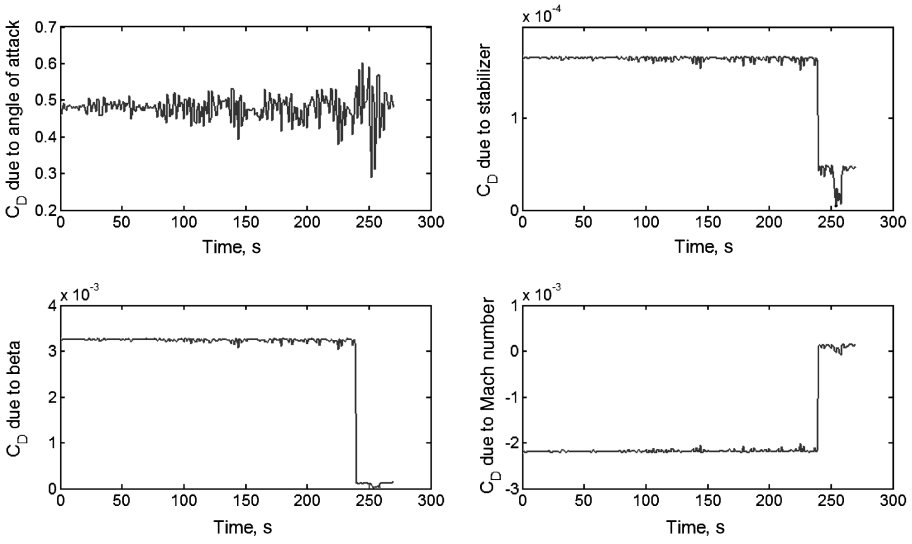

Fig. 5 Some of the drag-coefficient-related aerodynamic derivatives estimated by RBFNN.

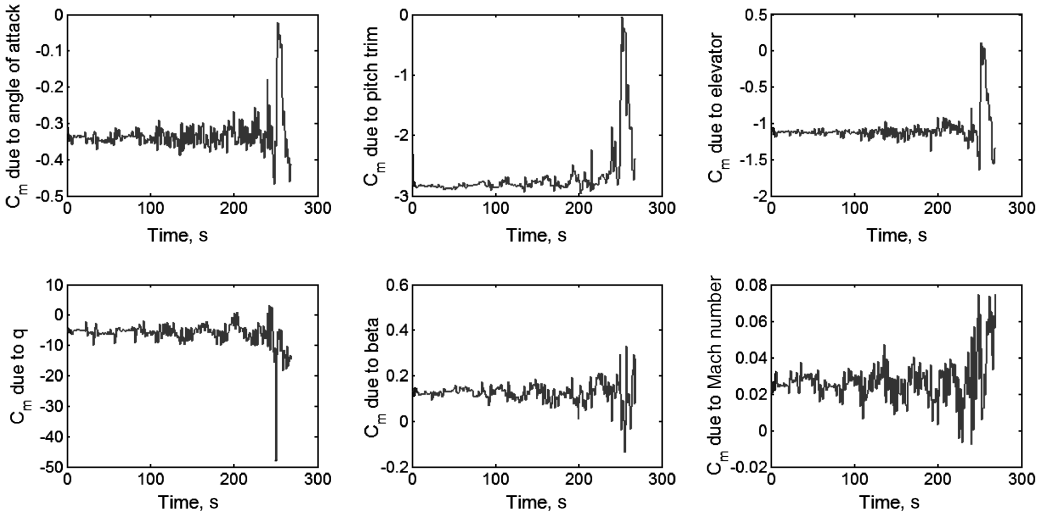

Fig. 6 Some of the pitching-moment-coefficient-related aerodynamic derivatives estimated by RBFNN.

the aircraft at this moment, the motion from the pilot's control to the aircraft would be opposite of what is needed. In the worst situation, this phenomenon may cause pilot induced oscillation (PIO).

D. Aircraft Stability and Flight Handling Quality Analysis

The aerodynamic derivatives listed in Eq. (18) are based on the body axes. Except for the pitching moment derivatives, the aerodynamic force derivatives, estimating from the RBFNN in the present study, are based on the wind axes. Therefore, the lift and drag derivatives have to be transformed into the body axes. In addition, the derivatives due to w and $\dot{w}$ are replaced by the derivatives due to α and $\dot{\alpha}$ by using $\Delta\alpha = w/u_0$. In addition, the aerodynamic derivatives due to the axial velocity on the wind axes are functions of the aerodynamic force coefficient, the force coefficient derivatives with the Mach number, and the Mach number itself. For example, the lift derivative due to axial velocity is can be represented as follows:

$$\overset{o}{L}_u = \frac{\partial(1/2\rho u_0^2 S C_L)}{\partial u} = \rho u_o S C_L + \frac{1}{2}\rho u_o S \frac{1}{M_{a0}}\frac{\partial C_L}{\partial M_a} = \rho u_o S C_L + \frac{1}{2}\rho u_o S \frac{1}{M_{a0}} C_{L_{M_a}} \tag{26}$$

According to the definition of flight phases in flight handling quality, the subject aircraft in cruise conditions should belong to Category B. After obtaining the aerodynamic derivatives on the body axes, the undamped natural frequency and damping ratio can be obtained from Eq. (19) and plotted as shown in Fig. 7. The positive damping ratio in the present study represents the stable damping (Fig. 7b). Therefore, the eigenvalues of the short-period motion are on the left-hand side of the imaginary axis, and the aircraft short-period mode is stable in the atmospheric turbulence. Before encountering turbulence, the average value of undamped natural frequency is 2.01 rad/s, and the average value of the damping ratio is 0.334. In the present atmospheric turbulence, the variation of undamped natural frequency ranges from 0.43 to 2.55 rad/s, and the damping ratio ranges from 0.09 to 1.42. Referring to the thumbprint, Fig. 7c, when the aircraft is in the turbulence under consideration, the flight handling quality during this period of time is unacceptable because of the low undamped frequency or damping ratio [18].

Figure 8 consists of 1) the CAP and damping ratio of short-period mode, and 2) the undamped natural frequency and normal load factor per unit angle of attack. Before encountering the turbulence, the average vaule of CAP is 0.387 $g^{-1} \cdot s^{-2}$, and the average value of normal load factor per unit angle of attack is 17.51 g/rad. The flight handling quality belongs to Level 1 based on CAP and n_α. The Level 1 flight handling quality means the flight situation is clearly adequate for the mission flight phase. When encountering the atmospheric turbulence, the CAP ranges from 2.21 to 0.13 $g^{-1} \cdot s^{-2}$, and the value of n_α ranges from 0.186 to 22 g/rad. When the CAP is 0.13 $g^{-1} \cdot s^{-2}$,

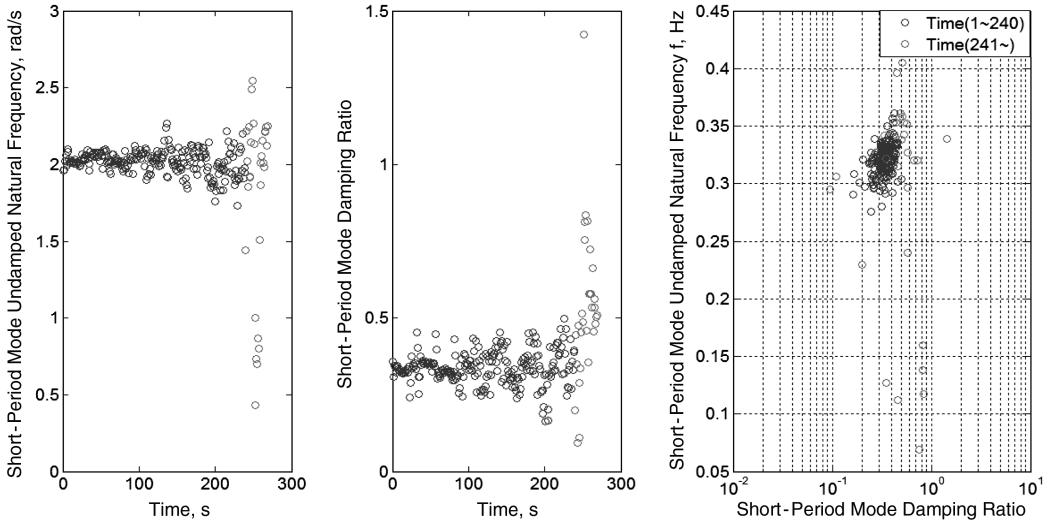

Fig. 7 Short-period longitudinal motion: a) undamped natural frequency, b) damping ratio, and c) thumbprint of criteria.

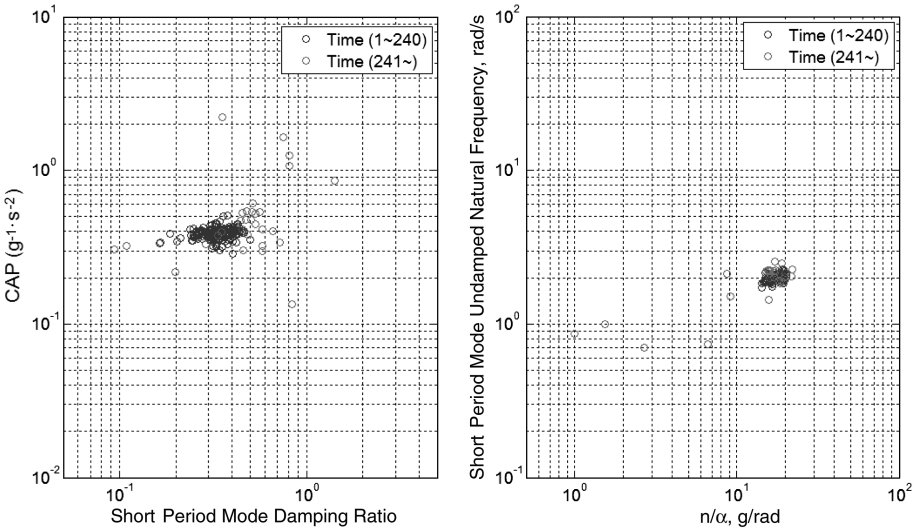

Fig. 8 Short-period mode: a) combining CAP and damping ratio, and b) undamped natural frequency and normal load factor per unit angle of attack.

the damping ratio is 0.198. The flight handling quality belongs to Level 3 and is very close to Level 2. When n_α is 6.62 g/rad, the undamped natural frequency is 0.736 g/rad. The worst flight handling quality situation for this case is with the handling quality belonging to Levels 2 and 3. Level 2 is adequate to accomplish the mission, but it increases the pilot workload. Level 3 flight handling quality means the aircraft is still controllable, but has inadequate mission effectiveness, and may cause high workload for pilots.

V. Conclusions

From the results of the analysis, the severe atmospheric turbulence caused degradation in aerodynamics, static stability, dynamic stability, and flight handling quality. The aerodynamic degradation in $C_{L\alpha}$ was up to 90% and the static stability $C_{m\alpha}$ was up to 96% compared to the normal flight in cruise conditions. The most significant finding in this case was the control power reduction of the control surfaces, including the stabilizer and elevator. In particular, the lift coefficient derivative with the stabilizer was decreased up to 99%. In addition, the sign change of $C_{m\delta e}$ implied a complete opposite phase lag of elevator control. Although the dynamic characteristics for the aircraft was still stable in the short-period mode, the flight handling quality was degraded to Level 3. These results imply that the aircraft in atmospheric turbulence was difficult to control in the short-period mode. This condition only lasted for several seconds. These findings were consistent with the flight operation manual for pilots, in which the instruction for pilots encountering turbulence at high altitude is that the elevator control should not be exercised. In this case, if the pilot applied the control force to the aircraft under severe turbulence, the unexpected delay and reversed control from the elevator might occur and could induce PIO. This would create a plunging and bumping motion.

Acknowledgments

This work is supported by the National Science Council and the Aviation Safety Council of Taiwan (no. NSC97-3114-P-707-001-Y).

References

[1] "In-Flight Icing Encounter and Crash into the Sea Transasia Airways Flight 791," Aviation Safety Council Aircraft Accident Report ASC-AOR-05-04-001, Taipei, April 2005.

[2] Buck, B. K., Bowles, R. L., and Newman, R. A., "Aircraft Acceleration Prediction with Flight Data Validation Due to Atmospheric Disturbance," AIAA Paper 2005-232, 2005.

[3] Pollak, J., and Lan, C. E., "Calculated Effect of Freestream Turbulence on Aerodynamic Characteristics of a Delta Wing," *AIAA Journal*, Vol. 33, No. 9, 1995, pp. 1734–1736. doi:10.2514/3.12717

[4] Peyada, N. K., and Ghosh, A. K., "Aircraft Parameter Estimation Using Neural Network Based Algorithm," AIAA Paper 2009-5941, 2009.

[5] Working Group 50, "Minimum Operational Performance Specification for Crash Protected Airborne Recorder Systems," European Organization for Civil Aviation Equipment, ED-112, Paris, 27 Jan. 2003.

[6] Iliff, K. W., and Taylor, L. W., "Determination of Stability Derivatives from Flight Data Using a Newton-Raphson Minimization Technique," NASA H-626, 1972.

[7] Iliff, K. W., "Aircraft Parameter Estimation," NASA H-1394, 1987.

[8] Hui, K., Auriti, L., and Ricciardi, J., "Advances in Real-Time Aerodynamic Model Identification," *Journal of Aircraft*, Vol. 42, No. 1, 2005, pp. 73–79. doi:10.2514/1.4501

[9] Weng, C. T., Ho, C. S., Lan, C. E., and Guan, M., "Aerodynamic Analysis of a Jet Transport in Windshear Encounter During Landing," *Journal of Aircraft*, Vol. 43, No. 2, 2006, pp. 419–427. doi:10.2514/1.15605

[10] Minkler, G., and Minkler, J., *Theory and Applications of Kalman Filtering*, Magellan Book Co., Palm Bay, FL, 1993.

[11] Yang, M. H., Chang K. C, Guan, M., Ho, C. S., and Hsiao, F. B., "Applied Flight Data to Analyse the Aircraft Encounter Turbulence," *2006 AASRC/CCAS Joint Conference on Disk* [CD-ROM], Aeronautical and Astronautical Society of the Republic of China, Taichung, Republic of China, 2006.

[12] "Instructions for Air-Reporting by Voice Communications," International Civil Aviation Organization, Doc. 4444, Appendix 1, Montreal, 2005.

[13] Mattingly, J. D., *Elements of Gas Turbine Propulsion*, McGraw–Hill, New York, 1996, pp. 213–337.

[14] Suykens, J. A. K., Vandewalle, J., and De Moor, B. L. R., *Artificial Neural Networks for Modeling and Control of Non-Linear Systems*, Kluwer Academic, Boston, 1996.

[15] Gupta, M. M., Jin, L., and Homma, N., *Static and Dynamic Neural Networks: From Fundamentals to Advanced Theory*, Wiley, Hoboken, NJ, 2003.

[16] Cook, M. V., *Flight Dynamics Principles*, Butterworth–Heinemann, Oxford, 1997, pp. 2–275.

[17] Nelson, R. C., *Flight Stability and Automatic Control*, McGraw–Hill, Singapore, 1998, pp. 96–179.

[18] Hodgkinson, J., *Aircraft Handling Quality*, Blackwell Science, Oxford, 1999, pp. 54, 56.